Calculation of the superconducting parameter $\langle I^2 \rangle$ for hcp transition metals

C.-G. Jiang, G. Fletcher,* and J. L. Fry
Department of Physics, Box 19059, The University of Texas at Arlington, Arlington, Texas 76019

D. A. Papaconstantopoulos
Complex Systems Theory Group, Naval Research Laboratory, Washington, D.C. 20375-5000
(Received 14 January 1991; revised manuscript received 1 April 1991)

The Fermi-surface-averaged electron-phonon interaction $\langle I^2 \rangle$ has been computed for 12 hexagonal-close-packed transition metals in the 3*d*, 4*d*, and 5*d* series. The calculations were first done with a quasiorthogonal tight-binding formalism based on Fröhlich's modified tight-binding wave function. This method employed accurate Slater-Koster fits to scalar-relativistic augmented-plane-wave band structures, and scaling laws to determine gradients of Slater-Koster parameters. The second method employed the rigid-muffin-tin approximation and the augmented-plane-wave band structures. The two methods gave the same systematic trends across the series and good agreement between computed values for most elements. Differences in some cases are attributed to sensitivity of the calculation to band-structure parameters and different approximations employed. The two results were compared with empirically deduced values and other theoretical calculations. Single-atomic character, crystal structure, and the area and complexity of the Fermi surface have been found to be important in determining the behavior of $\langle I^2 \rangle$.

I. INTRODUCTION

There has been considerable interest in predicting and calculating the superconducting transition temperature, T_c, for simple metals, transition metals, and their compounds since the BCS theory[1] and the more general Eliashberg-Nambu strong-coupling theory[2,3] were developed. Both of these theories relate closely properties of the superconducting state to those of the normal state (e.g., phonon spectrum, electron-phonon interaction, etc.). Therefore, the calculations of T_c depend sensitively on the properties of a material, and more accurate treatment of these normal-state properties gives a reliable determination of T_c.

T_c, in strong-coupling theory, is determined simply by solving the linearized Eliashberg equation to obtain the point where the nonzero solution of the gap function $\Delta(\omega)$ just appears. This is usually accomplished by an iterative numerical solution of Eliashberg's gap equation from knowledge of the Eliashberg electron-phonon coupling function, $\alpha^2(\omega)F(\omega)$, and the Coulomb repulsive potential, U_C. For simple metals falling in the weak-coupling regime, $\alpha^2(\omega)F(\omega)$ can be written in terms of pseudopotential form factors[4] and then the problem can be solved from the deduced gap edge $\Delta(\Delta_0)=\Delta_0$ by using the BCS relation $\Delta_0=1.76k_BT_c$. Alternatively, McMillan has done a detailed study of the dependence of T_c on the electron-phonon interaction in metals.[5] He used an iterative technique to improve the accuracy of an assumed analytic solution to the Eliashberg equation and found a simple formula for T_c in terms of three normal-state parameters:

$$T_c=\frac{\theta}{1.45}\exp\left[-\frac{1.04(1+\lambda)}{\lambda-\mu^*(1+0.62\lambda)}\right]. \quad (1)$$

In this equation, θ is the Debye temperature, and λ and μ^* are the electron-phonon and electron-electron coupling constants, respectively. Allen and Cohen[6] have performed pseudopotential calculations for λ and hence T_c from McMillan's equation (1) for 16 simple metals and the alkaline earths, Ca, Sr, and Ba. They concluded that the electron-phonon interaction mechanism does a completely adequate job of explaining T_c in these metals. For transition metals McMillan showed that the electron-phonon coupling constant, λ, can be written in the form of an electronic term divided by a phonon term:[5]

$$\lambda=\frac{n(E_F)\langle I^2\rangle}{M\langle\omega^2\rangle}, \quad (2)$$

where $n(E_F)$ is the density of states at the Fermi level E_F, $\langle I^2 \rangle$ is the square of the electronic transition matrix element averaged over the Fermi surface, M is atomic mass, and $\langle \omega^2 \rangle$ is the renormalized phonon frequency. By using Eqs. (1) and (2), and known values of $n(E_F)$, M, and $\langle \omega^2 \rangle$ for a given material, we can either determine an empirical value of $\langle I^2 \rangle$ through the empirical value of λ obtained via the experimentally measured value of T_c, or determine T_c through the value of λ by calculating the quantity $\langle I^2 \rangle$. The determination of the theoretical value of $\langle I^2 \rangle$ is therefore the major part of the task to determine T_c theoretically. The purpose of this paper is to obtain $\langle I^2 \rangle$ for hcp elements. Two basic techniques which have been used in calculating $\langle I^2 \rangle$ are the rigid-muffin-tin approximation (RMTA) and the modified-tight-binding approximation (MTBA). Both are used here to provide not only values of $\langle I^2 \rangle$, but also esti-

mates of their accuracy obtained by comparing the two results.

The RMTA was proposed by Gaspari and Gyorffy,[7] and is based on the Bloch formulation[8] of the electron-phonon interaction in which the transition matrix between two electron states is taken between eigenfunctions of the periodic potential. The systematic study of 3*d*, 4*d*, and 5*d* transition-metal series using the RMTA has been done by several previous researchers in cubic structures.[9–12] The MTBA technique was first implemented by Mitra[13] and Barišić *et al.*[14] All the effects of the electron-phonon interaction are represented by an electron-phonon interaction matrix taken between Fröhlich's modified-tight-binding bases.[15,16] In the case of transition metals the electrons are tightly bound, with wave functions describable by localized orbitals having nearly vanishing overlap with their nearest neighbors, and the transitions are between two states on the Fermi surface. These two approaches are identical to first order in the ion displacement.[17,18]

Fröhlich's modified-tight-binding basis leads[13,14] to the expression of transition matrix elements in terms of a gradient of Hamiltonian matrix elements in atomic bases $\nabla\langle\phi_m(\mathbf{r}-\mathbf{R}_i)|H|\phi_n(\mathbf{r}-\mathbf{R}_j)\rangle$. This allows use of the Slater-Koster (SK) simplified linear combinations of atomic-like orbitals (LCAO) scheme[19,20] to describe the variation of energy integrals due to lattice vibrations. By employing scaling laws for the SK bond parameters the gradient calculation may be simplified. Results for some cubic transition metals using the MTBA were given by Varma *et al.*;[21] Fry *et al.*[22] reported a systematic study of the cubic transition metals, and Fletcher *et al.*[23] computed $\langle I^2\rangle$ for several bcc transition metals and alloys.

While there is general agreement between values computed using the RMTA and the MTBA, some differences have been found which are thought to be due to the sensitivity of some of the calculations to numerical procedures and the details (shapes, sizes) of the Fermi surface. Since the RMTA and MTBA are both approximations, the regions of validity for these two may overlap but not be congruent. Direct comparison of computed values of $\langle I^2\rangle$ has been possible. Experimental values deduced through Eq. (1) are made uncertain by lack of reliable values of $\langle\omega^2\rangle$ and μ^*, so the agreement between the RMTA and MTBA is perhaps a better indication of the reliability of theoretical estimates of $\langle I^2\rangle$.

Until now the MTBA has been limited to cubic systems only. This paper reports calculations of $\langle I^2\rangle$ for 12 hcp transition metals using the MTBA and RMTA methods. The plan of this paper is the following. In Sec. II, we describe the quasiorthogonal, tight-binding formulation of the electronic transition matrix in an LCAO representation using the modified-tight-binding bases. The final MTBA expression for $\langle I^2\rangle$ in terms of transition matrix elements is presented. In the same section we also give a brief account of the RMTA approach. In Sec. III we present our computed values of $\langle I^2\rangle$, compare with previous estimates, and discuss the variation of $\langle I^2\rangle$ across the 3*d*, 4*d*, and 5*d* transition-metal series of the Periodic Table. Section IV contains the concluding remarks.

II. METHODS OF CALCULATION

The form of McMillan's representation for λ given in Eq. (2) is still valid for the hcp structure (two atoms per unit cell) if M is the mass of a single atom and $n(E_F)$ is the total density of states per unit cell. It is our purpose to calculate the quantities $\langle I^2\rangle$ for hcp metals. We now describe two methods of calculation which are used in this work.

A. The modified-tight-binding approximation

Fröhlich's assumption suggests that the tight-binding wave function corresponding to the ions slightly displaced with distance $\mathbf{u}_{i\tau}$ from their equilibrium position $\mathbf{R}_i+\tau$ can be written in modified-tight-binding form,[15,16]

$$\Phi_{m\tau}(\mathbf{k},\mathbf{r})=(1/\sqrt{N})\sum_i e^{i\mathbf{k}\cdot(\mathbf{R}_i+\tau)}\phi_m(\mathbf{r}-\mathbf{R}_i-\tau-\mathbf{u}_{i\tau})\ . \tag{3}$$

Assuming that the atom's displacements $\mathbf{u}_{i\tau}$ are small and the quasiorthogonality relation for the atomic-like bases remains valid,

$$\langle\phi_m(\mathbf{r}-\mathbf{R}_i-\tau-\mathbf{u}_{i\tau})|\phi_n(\mathbf{r}-\mathbf{R}_j-\tau'-\mathbf{u}_{j\tau'})\rangle\simeq\delta_{ij}\delta_{\tau\tau'}\delta_{mn}\ . \tag{4}$$

We can write the Bloch-like electron state in the deformed lattice as

$$\Psi_{\mathbf{k}\mu}(\mathbf{r})=\frac{1}{\sqrt{N}}\sum_{n,\tau}A^{\tau}_{n\mu}(k)\Phi_{n\tau}(\mathbf{k},\mathbf{r})\ , \tag{5}$$

where $A^{\tau}_{n\mu}(\mathbf{k})$ are eigenfunctions and $\Phi_{n\tau}(\mathbf{k},\mathbf{r})$ are Bloch-like sums defined in (3). The electron-phonon interaction is normally described by the scattering of an electron in one of the above states by the lattice vibrations, leading to a transition to another such state. Using (3), (4), and (5), one can show that the electronic transition matrix which is required in the calculation of $\langle I^2\rangle$ can be written in each Cartesian direction α as[13,20]

$$I^{\alpha}_{\mathbf{k}'\mu',\mathbf{k}\mu}=\sum_{m,n}A^{*}_{m\mu}(\mathbf{k})[\gamma^{\alpha}_{mn}(\mathbf{k})-\gamma^{\alpha}_{mn}(\mathbf{k}')]A_{n\mu'}(\mathbf{k}')\ , \tag{6}$$

where

$$\gamma^{\alpha}_{mn}(\mathbf{k})=\sum_{i,j}[\nabla_{\alpha}\langle\phi_m(\mathbf{r}-\mathbf{R}_i-\tau)|H|\phi_n(\mathbf{r}-\mathbf{R}_j-\tau')\rangle]\times e^{i\mathbf{k}\cdot(\mathbf{R}_i+\tau-\mathbf{R}_j-\tau')}\ . \tag{7}$$

The energy integrals in (7) are sums of terms that are products of angular parts (functions of the direction cosines l,m,n of $\mathbf{R}_i+\tau$) and radial parts (SK bond parameters, which are functions of distance between two atoms). Therefore, to calculate (7) we shall write the gradient operator ∇_{α} in terms of derivatives of the energy integrals with respect to radial distance and direction

cosines. For the evaluation of the radial derivatives one must know the bond length dependence of each of the bond strength parameters. In this study, we have used the empirical scaling laws obtained by Harrison,[24] where one expresses the variation of the bond strength as an inverse power of the bond length, with the power depending only upon the angular symmetry of the orbitals involved. This has been found to be quite accurate, particularly in the vicinity of the equilibrium atomic position. A detailed analysis of the validity of this scaling law can be found in Ref. 24. According to Harrison's scaling law the *ss*, *pp*, and *sp* bonds are taken to vary as D^{-2}, the *dd* bonds as D^{-5}, and the *sd* and *pd* bonds as $D^{-3.5}$, where D is bond length. For hcp structures, the work to evaluate (6) and (7) is very tedious, so we have used artificial intelligence programming to carry out this task accurately.

The quantity $\langle I^2 \rangle$ can be written as

$$\langle I^2 \rangle = \frac{\sum_{\mu,\mu'} \int_{\mathrm{FS}} \frac{dS_{\mathbf{k}}}{|\nabla_{\mathbf{k}} E_{\mathbf{k}\mu}|} \int_{\mathrm{FS}} \frac{dS_{\mathbf{k}'}}{|\nabla_{\mathbf{k}'} E_{\mathbf{k}'\mu'}|} \sum_{\alpha} |I^{\alpha}_{\mathbf{k}'\mu',\mathbf{k}\mu}|^2}{\left[\sum_{\mu} \int_{\mathrm{FS}} \frac{dS_{\mathbf{k}}}{|\nabla_{\mathbf{k}} E_{\mathbf{k}\mu}|} \right]^2} . \tag{8}$$

Substituting (6) and (7) into (8), and using symmetry relations like $\gamma^{\alpha *}_{mn} = -\gamma^{\alpha}_{nm}$, we find the final expression for $\langle I^2 \rangle$ in an LCAO representation

$$\langle I^2 \rangle = \frac{4 \sum_{m<n} \sum_{\alpha} a^{\alpha}_{mn} + 2 \sum_{m} b_m}{\left[\sum_{\mu} \int_{\mathrm{FS}} \frac{dS_{\mathbf{k}}}{|\nabla_{\mathbf{k}} E_{\mathbf{k}\mu}|} \right]^2} , \tag{9}$$

where

$$a^{\alpha}_{mn} = \sum_{\mu} \int_{\mathrm{FS}} \frac{dS_{\mathbf{k}}}{|\nabla_{\mathbf{k}} E_{\mathbf{k}\mu}|} \sum_{m',n'} A^{*}_{m'\mu}(\mathbf{k}) A_{n'\mu}(\mathbf{k}) \gamma^{\alpha}_{m'm}(\mathbf{k}) \gamma^{\alpha *}_{n'n}(\mathbf{k}) \sum_{\mu'} \int_{\mathrm{FS}'} \frac{dS_{\mathbf{k}'}}{|\nabla_{\mathbf{k}'} E_{\mathbf{k}'\mu'}|} A^{*}_{m\mu'}(\mathbf{k}') A_{n\mu'}(\mathbf{k}')$$
$$- \sum_{\mu} \int_{\mathrm{FS}} \frac{dS_{\mathbf{k}}}{|\nabla_{\mathbf{k}} E_{\mathbf{k}\mu}|} \sum_{m'} A^{*}_{m\mu}(\mathbf{k}) A_{m'\mu}(\mathbf{k}) \gamma^{\alpha *}_{m'n}(\mathbf{k}) \sum_{\mu'} \int_{\mathrm{FS}'} \frac{dS_{\mathbf{k}'}}{|\nabla_{\mathbf{k}'} E_{\mathbf{k}'\mu'}|} \sum_{m'} A_{m'\mu'}(\mathbf{k}') A^{*}_{n\mu'}(\mathbf{k}') \gamma^{\alpha}_{mm'}(\mathbf{k}') \tag{10}$$

and

$$b_m = \sum_{\mu} \int_{\mathrm{FS}} \frac{dS_{\mathbf{k}}}{|\nabla_{\mathbf{k}} E_{\mathbf{k}\mu}|} \sum_{m',n',\alpha} A^{*}_{m'\mu}(\mathbf{k}) A_{n'\mu}(\mathbf{k}) \gamma^{\alpha}_{m'm}(\mathbf{k}) \gamma^{\alpha *}_{n'm}(\mathbf{k}) \sum_{\mu'} \int_{\mathrm{FS}'} \frac{dS_{\mathbf{k}'}}{|\nabla_{\mathbf{k}'} E_{\mathbf{k}'\mu'}|} \left| A_{m\mu'}(\mathbf{k}') \right|^2$$
$$+ \left[\sum_{\mu} \int_{\mathrm{FS}} \frac{dS_{\mathbf{k}}}{|\nabla_{\mathbf{k}} E_{\mathbf{k}\mu}|} \sum_{m',\alpha} A_{m'\mu}(\mathbf{k}) A^{*}_{m\mu}(\mathbf{k}) \gamma^{\alpha}_{mm'}(\mathbf{k}) \right]^2 . \tag{11}$$

In order to do the numerical evaluation of these surface integrals, we have divided the $\frac{1}{24}$th irreducible Brillouin zone (IBZ) into 384 tetrahedra. By checking the relation between Fermi energy and those energies of k points at four vertices of each tetrahedron, we have constructed the Fermi surface in the hcp Brillouin zone and have performed surface integrations over the Fermi surface using the analytic tetrahedron method (ATM).[25]

B. The rigid-muffin-tin approximation

The assumption that the muffin-tin potential moves rigidly with the atom as it vibrates is known as the rigid-muffin-tin approximation (RMTA). The RMTA was applied by Gaspari and Gyorffy[7] to derive a now widely used formula for the electron-ion matrix element $\langle I^2 \rangle$, i.e.,

$$\langle I^2 \rangle = \frac{2E_F}{\pi^2 n^2(E_F)} \sum_{l} (l+1) \sin^2(\delta_{l+1} - \delta_l) R_l R_{l+1} , \tag{12}$$

where δ_l is the scattering phase shift at E_F and R_l is the ratio

$$R_l = \frac{n_l(E_F)}{n_l^{(1)}(E_F)} , \tag{13}$$

where $n_l(E_F)$ are the angular momentum components of the density of states (DOS) at E_F within the muffin-tin sphere and $n_l^{(1)}(E_F)$ is the single scatterer DOS which can be computed from the radial wave functions. The above equation is exact to $l=1$, but for $l=2$ and higher it involves nonspherical corrections. These corrections, as shown by Butler *et al.*,[26] are small for cubic elements. For the hcp elements we also expect the nonspherical corrections to be small and hence we have neglected them in this work.

The necessary input to the Gaspari-Gyorffy formula was generated as follows: (a) the phase shifts δ_l were found from the logarithmic derivatives of the radial wave functions that correspond to the self-consistent crystal

potential that we found from an APW calculation of each element. (b) The DOS $n(E_F)$ and $n_l(E_F)$ were computed by the tetrahedron method[25] based on APW results for 45 **k** points in the irreducible hcp Brillouin zone. (c) The free scatterers $n_l^{(1)}(E_F)$ were calculated using the radial wave functions of the above crystal potential.

Finally, the accuracy of the RMTA has been questioned, especially for the new high-temperature ionic superconductors. However, in the hcp *d*-like elements that we examine here the RMTA should work well. Comparison with tight-binding results, where the RMTA is not necessarily made, provides a test of both approximation methods, and is given in the next section.

III. RESULTS AND DISCUSSION

A. Band structures

The MTBA and RMTA formulas for $\langle I^2 \rangle$ have been applied here to all hcp metals in the 3*d*, 4*d*, and 5*d* transition-metal series. The first-principles band structures were self-consistent, scalar-relativistic calculations performed by the APW method at the equilibrium lattice constants. The SK fits to these band structures may be found in Ref. 27. In the MTBA work we employed only the two-centered (2C) orthogonal parameters in order to simplify the process, so comparison of computed quantities for RMTA and MTBA methods must be made with this fact in mind. The 2C-nonorthogonal SK parameters are more accurate, with a typical rms error of 5 mRy over the APW bands, while the rms error using orthogonal parameters is approximately 10 mRy. The SK parameters, band structures, and $n(E)$ plots are presented in Ref. 27, along with rms errors of the various fits.

Results for the calculation of the electron-phonon interaction sometimes depend sensitively upon the shape of bands, the Fermi energy and Fermi surface, and $n(E_F)$, so accurate determination of these quantities is important. Table I shows E_F and $n(E_F)$ for the orthogonal-tight-binding (OTB), nonorthogonal-tight-binding (NOTB), and APW band structures for each element considered here. Integrals with the OTB and NOTB band structures were computed here using the ATM with 384 and then 1536 tetrahedra in the IBZ. The APW results were obtained using only 45 **k** points in the IBZ, since generation of many points was not practical for a systematic study of the hcp elements. Because of this, some of the computed values were not stable and are left blank in Table I in the APW columns. E_F and $n(E_F)$ have also been computed independently with a different ATM program and 3078 tetrahedra in the IBZ.[28] In view of the different numbers of tetrahedra used, we consider agreement between the two NOTB results excellent (see Ref. 28 for more details).

The Fermi energies computed by all these methods agree well, but $n(E)$ is a rapidly varying quantity near E_F for some of the hcp metals, so greater differences occur for $n(E_F)$ with the different band structures. Using the NOTB values as a standard (better ATM calculations, better fit to first-principles band structures), the average absolute difference is about 15% for both the OTB and APW values of $n(E_F)$, with a maximum difference of about 36% for Y, where the APW DOS may not be reliable due to the small number of **k** points used. Since values of $\langle I^2 \rangle$ quoted below were obtained with APW and OTB band structures, a significant comparison is the corresponding $n(E_F)$ values for each element obtained from these bands. The average absolute difference is 17% between APW and OTB computed $n(E_F)$, with a maximum difference of about 70%, again for Y.

TABLE I. Fermi energy and density of states for hcp elements. The second column gives the c/a ratio for each metal, the third through fifth columns show the computed Fermi energies for the orthogonal-tight-binding (OTB), nonorthogonal-tight-binding (NOTB), and augmented-plane-wave (APW) band structures of Ref. 27 of the text, and the sixth through eighth columns give the corresponding values for the density of states at the Fermi energy, $n(E_F)$. The ninth column gives $n(E_F)$ computed independently in Ref. 28 of the text for the same NOTB band structures used here.

		E_F (Ry)			$n(E_F)$ (states/Ry unit-cell)			
Element	c/a	OTB	NOTB	APW	OTB	NOTB	APW	Ref. 28
Sc	1.59	0.429	0.430	0.427	57.1	61.4	74.7	61.0
Ti	1.59	0.590	0.590	0.592	26.7	23.4	28.9	24.0
Co	1.62	0.683	0.683	0.681	85.2	78.6	74.4	
Zn	1.86	0.404	0.386		9.1	10.3		
Y	1.57	0.395	0.398	0.394	52.0	60.1	82.0	60.8
Zr	1.59	0.544	0.545	0.542	26.9	22.1	22.7	
Tc	1.61	0.747	0.740	0.737	22.5	25.6	24.4	25.4
Ru	1.59	0.762	0.758	0.754	25.4	22.1	24.3	22.0
Cd	1.89	0.190	0.250		12.4	15.1		11.4
Hf	1.58	0.574	0.575	0.575	25.1	17.4	21.7	17.2
Re	1.62	0.800	0.786	0.783	17.7	19.0	18.3	20.0
Os	1.58	0.850	0.834	0.833	18.6	17.1	18.4	16.8

B. Computed values of $\langle I^2 \rangle$

Calculation of $\langle I^2 \rangle$ in the MTBA is more expensive than calculation of $n(E_F)$ since matrix elements are complicated and whole zone integration is required. Consequently the ATM was limited to 384 tetrahedra in each of the 24 IBZ, i.e., 9216 tetrahedra in the whole zone. On the other hand the RMTA calculation of $\langle I^2 \rangle$ employed the same 45 **k** points as the $n(E_F)$ calculation. We report in Table II our results for $\langle I^2 \rangle$using both MTBA and RMTA methods, together with the empirical values for some of the elements from the studies of Hopfield[29] and Butler.[9] The empirical values were obtained by multiplying empirical values of λ (which required experimental estimates of T_c and μ^*) by $M\langle \omega^2 \rangle$ and dividing by $n(E_F)$. Consequently, substantial uncertainty is associated with the empirical values of $\langle I^2 \rangle$ because they depend upon the poorly known values of the Coulomb pseudopotential μ^*, and on estimates of $\langle \omega^2 \rangle$. Details of the procedures used in estimating these quantities may be found in Refs. 9 and 29. Also listed in Table II are other RMTA calculations, including those by Butler[9] (4*d*) and Papaconstantopoulos *et al.*[10] (3*d* and 4*d*) for hcp metals in equal density fcc or bcc structures and John *et al.*[11] (5*d*) in the hcp structure. The latter work included spin-orbit corrections to the Gaspari-Gyorffy RMTA formula, but was based on non-self-consistent band-structure calculations.

The principal results of this paper are contained in the second and third columns of Table II. Both are theoretical calculations of $\langle I^2 \rangle$ for hcp metals using no adjustable parameters, but employing the MTBA and RMTA, respectively. Even if the MTBA and RMTA approximations were identical in principle, the limited numerical convergence and some different approximations being made in deriving the final expressions of $\langle I^2 \rangle$ of the two calculations would be expected to produce some differences. Thus we feel that reasonable agreement between the two techniques has been achieved, and note that the same systematic trends through the Periodic Table have been found. In fact a comparison of the % difference between RMTA and MTBA values of $n(E_F)$ and the % difference between corresponding values of $\langle I^2 \rangle$ shows a strong correlation. We note that on the average $\langle I^2 \rangle_{\mathrm{RMTA}}$ is about 25% less than $\langle I^2 \rangle_{\mathrm{MTBA}}$. Thus there are noticeable systematic differences. The largest discrepancies for $\langle I^2 \rangle$ occur near the first of each transition series: 55% for Sc and Y, followed by 25% for Ti, Zr, and Hf, where sharp structure of the DOS near E_F makes the RMTA results less reliable because of the limited number of **k** points used. These follow the same pattern as the corresponding $n(E_F)$. We can offer no explanation for the systematic shift at this time, but attribute the correlated larger discrepancies to the numerical sensitivity of the calculations in some of the elements.

TABLE II. Fermi-surface-averaged electron-phonon interaction, $\langle I^2 \rangle$, for hcp transition metals. The second and third columns give $\langle I^2 \rangle$ for the modified-tight-binding (MTBA) and rigid-muffin-tin (RMTA) approximations obtained here. The fourth column shows empirical estimates made elsewhere, and the sixth and seventh columns show the corresponding theoretical values for bcc and fcc phases of the metals obtained from earlier RMTA calculations.

			$\langle I^2 \rangle$ (Ry^2/a.u.^{2})		
Element	hcp MTBA	hcp RMTA	Empirical estimates	bcc RMTA	fcc RMTA
Sc	0.0032	0.0014		0.0042[c]	
Ti	0.0050	0.0038	0.0077[a]		0.0080[c]
Co	0.0026	0.0022			0.0060[c]
Zn	0.0058				0.0052[c]
Y	0.0033	0.0015	0.0008[b]	0.0021[b]	0.0044[c]
Zr	0.0061	0.0046	0.0098[a]	0.0070[b]	
			0.0082[b]	0.0122[c]	
Tc	0.0135	0.0111	0.0244[b]	0.0189[b]	0.0212[c]
Ru	0.0122	0.0110	0.0167[b]	0.0116[b]	0.0141[b]
					0.0181[c]
Cd	0.0032				0.0030[c]
Hf	0.0076	0.0056			
		0.0074[d]			
Re	0.0183	0.0143			
		0.0124[d]			
Os	0.0189	0.0170			
		0.0123[d]			

[a]Hopfield, Ref. 29.
[b]Butler, Ref. 9.
[c]Papaconstantopoulos *et al.*, Ref. 10.
[d]John *et al.*, Ref. 11.

C. Systematic trends of $\langle I^2 \rangle$ in the Periodic Table

It is interesting and important to understand, at least in a qualitative way, how $\langle I^2 \rangle$ varies from one metal to another across the transition-metal series. The general trends for cubic metals have been established in previous studies[9-12,21-23] for the $3d$, $4d$, and $5d$ series. For the cubic metals there is good agreement between computed values of $\langle I^2 \rangle$ using RMTA and MTBA methods,[22] so, to reduce clutter, only RMTA cubic results are shown in the figures. A suggestive curve representing $\langle I^2 \rangle$ as an atomic property has been drawn in Fig. 2 for the $4d$ cubic transition metals to show the trends with atomic number. It is drawn through the points Y, Zr, and Ru where we believe from our calculations that the single atomic nature dominates the band features. This curve has been superimposed without change into Figs. 1 and 3, revealing approximately the same trend in each series: $\langle I^2 \rangle$ increases to a maximum as the d bands and overlapping s band become half-filled, followed by a corresponding decrease as both bands fill. The distribution is approximately symmetric about the half-filled configuration in the solid, $nd^5(n+1)s^1$ (i.e., Cr,Mo,W).

While $\langle I^2 \rangle$ data are more sparse for hcp metals, RMTA and MTBA points computed here may be interpreted approximately with the same universal curve used for the cubic transition metals. As a rule, hcp values of $\langle I^2 \rangle$ appear to be lower than cubic values, with the exception of some of the $5d$ transition metals. This may result from spin-orbit corrections employed in Ref. 11 or simply reflect the lack of self-consistency in the band structures in that calculation. It is difficult to deduce from formulas as complicated as Eqs. (9)–(11) (MTBA) or (12) and (13) (RMTA) how the observed trends occur, but we offer the following suggestions.

In the MTBA, band effects enter most strongly through the Fermi-surface shape and the density of states at the Fermi level [see Eq. (9)], while the atomic-like character is displayed through the gradients of 2C SK parameters which contain implicitly the effective atomic potentials. Unless unusual Fermi-surface-averaging effects occur, which may be the case for Tc, e.g., the electron-phonon coupling trends will be dominated by the gradients of the SK parameters which are expected to reflect the electron-hole symmetries about the atomic number corresponding to a half-filled shell. A similar separation of $\langle I^2 \rangle$ into band and atomic contributions occurs in the RMTA: Band effects appear in the partial and total DOS, while the scattering phase shift and single scatterer DOS may be dominated by the muffin-tin (atomic-like) potential.

Comparing our hcp results with the results of cubic RMTA calculations in cubic structures, we find several of the elements showing their $\langle I^2 \rangle$ values behaving as

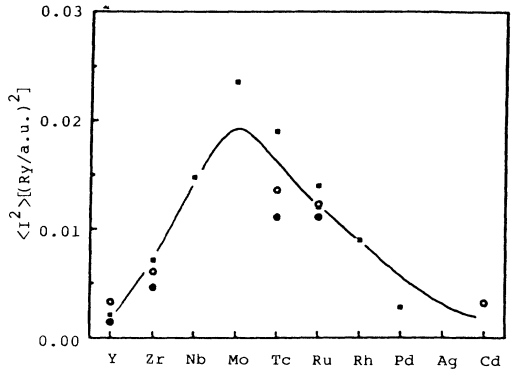

FIG. 2. $\langle I^2 \rangle$ in $4d$ transition metals. Open and solid circles are the results of the present hcp MTBA and RMTA studies, respectively. Solid squares are the cubic RMTA values from Ref. 9 of the text.

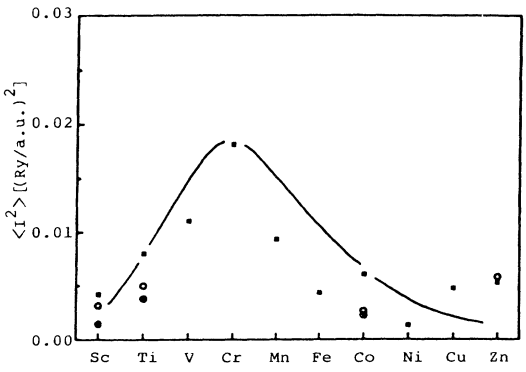

FIG. 1. $\langle I^2 \rangle$ in $3d$ transition metals. Open and solid circles are the results of the present hcp MTBA and RMTA studies, respectively. Solid squares are the cubic RMTA values from Ref. 10 of the text.

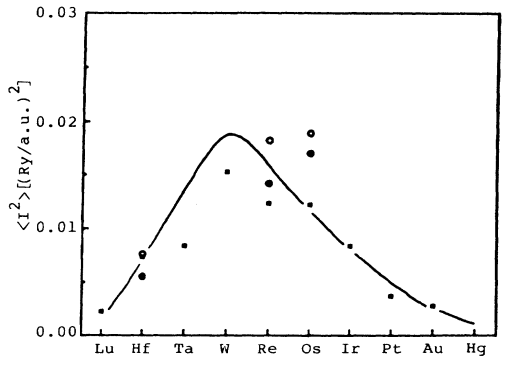

FIG. 3. $\langle I^2 \rangle$ in $5d$ transition metals. Open and solid circles are the results of the present hcp MTBA and RMTA studies, respectively. Solid squares are the RMTA values for hcp metals reported in Ref. 11 of the text.

atomic in nature, since there is very close agreement between hcp and cubic values. Butler[26] has done calculations for Ru both in bcc and fcc structures using the RMTA. The $\langle I^2 \rangle$ values of his calculations are 0.0116 and 0.0141 $Ry^2/a.u.^2$ for bcc and fcc phases, respectively, which are close to our hcp value of 0.0122 $Ry^2/a.u.^2$ This suggests that $\langle I^2 \rangle$ for Ru is strongly of single atomic character. The largest discrepancy found between our MTBA and RMTA bcc values is for Tc. This may be a consequence of the importance of band effects, as suggested in Ref. 30. We found the area of the Fermi surface of Tc to be the largest among the transition metals and very complicated, a factor which may account for the observed differences.

Since superconducting transition temperature T_c is influenced directly by the value of λ given by Eq. (2) it should be emphasized that the product $n(E_F)\langle I^2 \rangle$ is more directly connected to T_c. At this level the atomic in nature quantities $\langle I^2 \rangle$ are modulated by $n(E_F)$ which bring into the picture the different band-structure effects for different elements and crystal structures.

IV. CONCLUSION

We have computed the Fermi-surface-averaged electron-phonon interaction in hcp transition metals using the MTBA and RMTA expressions. While there is acceptable agreement between the two results, especially considering the various numerical constraints placed upon the calculations, the RMTA values were systematically lower by about 25%. Both methods found the same systematic trends across the Periodic Table which appear to be similar to the trends seen in the cubic metals. Exceptions to the trends are attributed to special Fermi-surface or band effects. Scalar-relativistic effects were included in the band structures, but explicit corrections to the RMTA and MTBA formulas were not made. The basic assumptions of the RMTA and MTBA are not necessarily the same. One uses a muffin-tin potential which is assumed to move rigidly during a lattice vibration, while the other makes no assumption about the form of the potential, but assumes scaling laws for the change in integrals of the potential. Additional computational details make it remarkable that the level of agreement found in Table II is possible, and suggest that we may have fairly reliable ($\pm 25\%$) theoretical estimates of $\langle I^2 \rangle$ for the transition metals. Since the MTBA method may more easily be extended to crystals with arbitrary numbers of atoms and arbitrary symmetry, agreement with the RMTA for hcp, bcc, and fcc metals suggests it as a method of choice for future studies in complex systems. New techniques[31] for measuring $\langle I^2 \rangle$ directly may further serve to check existing calculations and provide a better theoretical understanding of the electron-phonon interaction in metals.

ACKNOWLEDGMENTS

We would like to thank L.L. Boyer for making a modification of the density-of-states program used in the ATM calculations. Computational facilities were provided by The University of Texas Center for High Performance Computing. Work at The University of Texas at Arlington was supported by The Robert A. Welch Foundation under Grant No. Y-707.

*Present address: Department of Physics, Texas Tech University, Lubbock, TX 79409.

[1]J. Bardeen, L. N. Cooper, and J. R. Schrieffer, Phys. Rev. **106**, 162 (1975); **108**, 1175 (1957).
[2]G. M. Eliashberg, Zh. Eksp. Teor. Fiz. **38**, 966 (1960) [Sov. Phys.—JETP **11**, 696 (1960)].
[3]Y. Nambu, Phys. Rev. **117**, 648 (1960).
[4]J. P. Carbotte and R. C. Dynes, Phys. Rev. **172**, 476 (1968).
[5]W. L. McMillan, Phys. Rev. **167**, 331 (1968).
[6]P. B. Allen and M. L. Cohen, Phys. Rev. **187**, 525 (1969).
[7]G. D. Gaspari and B. L. Gyorffy, Phys. Rev. Lett. **25**, 801 (1972).
[8]F. Bloch, Z. Phys. **52**, 555 (1928).
[9]W. H. Butler, Phys. Rev. B **15**, 5267 (1977).
[10]D. A. Papaconstantopoulous, L. L. Boyer, B. M. Klein, A. R. Williams, V. L. Morruzzi, and J. F. Janak, Phys. Rev. B **15**, 4221 (1977).
[11]W. John, V. V. Nemoshkalenko, V. N. Antonov, and Vl. N. Antonov, Phys. Status Solidi B **121**, 233 (1984).
[12]D. G. Pettifor, J. Phys. F **7**, 1009 (1977).
[13]T. K. Mitra, J. Phys. C **2**, 52 (1969).
[14]S. Barišić, J. Labbé, and J. Friedel, Phys. Rev. Lett. **25**, 919 (1970).
[15]H. Fröhlich, in *Perspectives in Modern Physics,* edited by R. E. Marshak (Interscience, New York, 1966).
[16]H. Fröhlich and T. K. Mitra, J. Phys. C **1**, 548 (1968).
[17]R. A. Deegan, Phys. Rev. B **5**, 1183 (1972).
[18]J. Ashkenazi, M. Dacorogna, and M. Peter, Solid State Commun. **29**, 181 (1979).
[19]J. C. Slater and G. F. Koster, Phys. Rev. **94**, 1498 (1954).
[20]M. Miasek, Phys. Rev. **107**, 92 (1957).
[21]C. M. Varma, E. I. Blount, P. Vashishta, and W. Weber, Phys. Rev. B **19**, 6130 (1979).
[22]J. L. Fry, G. Fletcher, P. C. Pattnaik, and D. A. Papaconstantopoulos, Physica **135B**, 473 (1985).
[23]G. Fletcher, J. L. Fry, P. C. Pattnaik, D. A. Papaconstantopoulos, and N. C. Bacalis, Phys. Rev. B **37**, 4944 (1988).
[24]W. A. Harrison and S. Froyen, Phys. Rev. B **21**, 3214 (1980); S. Froyen and W. A. Harrison, *ibid.* **20**, 2420 (1979).
[25]G. Lehmann and M. Taut, Phys. Status Solidi **54**, 469 (1972); P. C. Pattnaik, J. L. Fry, N. E. Brener, and G. Fletcher, Int. J. Quantum Chem. Symp. **15**, 499 (1981).
[26]W. H. Butler, J. J. Olson, J. S. Faulkner, and B. L. Gyorffy, Phys. Rev. B **14**, 3823 (1976).

[27]D. A. Papaconstantopoulos, *Handbook of the Band Structures of Elemental Solids* (Plenum, New York,1986).
[28]B. A. Sanborn, P. B. Allen, and D. A. Papaconstantopoulos, Phys. Rev. B **40**, 6037 (1989).
[29]J. J. Hopfield, Phys. Rev. **186**, 443 (1969).
[30]R. Asokamani and K. Iyakutti, J. Phys. F **10**, 1157 (1980).
[31]S. D. Brorson, A. Kazeroonian, J. S. Moodera, D. W. Face, T. K. Cheng, E. P. Ippen, M. S. Dresselhaus, and G. Dresselhaus, Phys. Rev. Lett. **64**, 2172 (1990).